

# Valence quark contributions for the $\gamma N \rightarrow P_{11}(1440)$ form factors

G. Ramalho<sup>1</sup> and K. Tsushima<sup>2</sup>

<sup>1</sup>*Centro de Física Teórica e de Partículas, Av. Rovisco Pais, 1049-001 Lisboa, Portugal and*

<sup>2</sup>*Excited Baryon Analysis Center (EBAC) and Theory Center,  
Thomas Jefferson National Accelerator Facility, Newport News, VA 23606, USA*

(Dated: May 31, 2019)

Using a covariant spectator quark model we estimate valence quark contributions to the  $F_1^*(Q^2)$  and  $F_2^*(Q^2)$  transition form factors for the  $\gamma N \rightarrow P_{11}(1440)$  reaction. The Roper resonance,  $P_{11}(1440)$ , is assumed to be the first radial excitation of the nucleon. The present model requires no extra parameters except for those already fixed by the previous studies for the nucleon. Our results are consistent with the experimental data in the high  $Q^2$  region, and those from lattice QCD. We also estimate the meson cloud contributions, focusing on the low  $Q^2$  region, where they are expected to be dominant.

## I. INTRODUCTION

The structure of the  $P_{11}(1440)$  resonance, which will be referred to as "the Roper" in this article, has been a longstanding mystery. Its mass and large width are difficult to understand in a framework of quark models [1–4]. The decay branches imply that it is a mixture of  $\pi N$  and  $\pi\pi N$  states (dominated by the mixture of  $\pi\Delta$  and  $\sigma N$  channels). Recently, the precision data from CLAS at JLab [5] (single and double pion electroproduction), and a global analysis from MAID [6, 7] in the region  $Q^2 \leq 6 \text{ GeV}^2$  have become available. The extracted  $\gamma N \rightarrow P_{11}(1440)$  helicity amplitudes can give hints on the internal structure of the Roper. Indeed, the amplitudes (and the transition form factors) extracted from the experiments, turned out to show a surprising  $Q^2$  dependence.

In a simple quark model picture, the Roper can be regarded as the first radial excitation of the nucleon. Recent experimental data at large  $Q^2$  [5, 6] support this picture [4, 5, 8, 9]. In the high  $Q^2$  region ( $Q^2 > 2 \text{ GeV}^2$ ) the data is consistent with the predicted  $Q^2$  dependence of relativistic constituent and light-front quark models [4, 5, 8]. These models, however, fail to explain the lower  $Q^2$  data, particularly at the photon point,  $Q^2 = 0$ . This discrepancy has been interpreted as a manifestation of the missing meson cloud effects in the models [4, 8–10]. Unfortunately, the magnitude of the meson cloud contributions is less constrained, and they are more model dependent than the valence quark contributions, which are dominant at larger  $Q^2$ . (In general, the meson cloud contributions are expected to fall as  $Q^2$  increases.) In this study, we estimate the meson cloud contributions using a covariant spectator constituent quark model which is consistent with the large  $Q^2$  region data of the CLAS. The present model requires no extra parameters except for those already fixed by the previous studies for the nucleon [11].

The  $\gamma N \rightarrow P_{11}(1440)$  transition amplitudes have been

studied in several ways: treating the Roper as a quark-gluon system [12], a pure valence quark system [4, 13–18], and a valence quark system dressed by  $q\bar{q}$  pairs [19–23]. Relativity has been proven to be very important, not only for a large  $Q^2$ , but also for the region  $Q^2 \sim 0$ . It may even decide the sign of the amplitudes near  $Q^2 = 0$  [4, 5, 13, 14]. The nucleon to Roper transition amplitudes have been also studied using dynamical baryon-meson coupled-channel models. They usually treat the baryons and mesons as effective degrees of freedom, and the baryons are dressed with a meson cloud nonperturbatively. (For details, see e.g., Refs. [10, 24–32] and a review [33].) The non-valence quark degrees of freedom was also introduced by coupling the pion and other meson fields to the valence quarks [34–36]. The  $\gamma N \rightarrow P_{11}(1440)$  transition was also studied in lattice QCD [37].

In this study we compute the  $\gamma N \rightarrow P_{11}(1440)$  transition form factors using a valence quark model based on the covariant spectator formalism [38]. Relativity is implemented consistently. In this model a baryon is described as a quark-diquark system, where the diquark has all possible polarizations (spin state 0 or 1) and acts as a spectator. The isolated quark in the baryon interacts with the photon in the impulse approximation. The model has been applied successfully for the studies of spin 1/2 and spin 3/2 low-lying baryons [11, 39–44]. We assume that the Roper is the first radial excitation of the nucleon, which also ensures that it is orthogonal to the nucleon (valence quark) state. Using a model with no extra new adjustable parameters, we compute the  $Q^2$  dependence of the transition form factors. We find an excellent agreement with the data [5, 6] in the high  $Q^2$  region. Furthermore, we extend the model to a lattice QCD regime and compare with the lattice data for a large pion mass ( $m_\pi = 720 \text{ MeV}$ ), and find also a good agreement, particularly in the low  $Q^2$  region,  $Q^2 < 1 \text{ GeV}^2$ . Note that under the two conditions, high  $Q^2$  and lattice simulations with heavy pions, meson cloud effects

are expected to become small or negligible [45]. The two agreements mentioned above, support that the present model can describe well the valence quark contributions. Encouraged by the successful features of the model, we estimate the meson cloud contributions focusing on the low  $Q^2$  region.

This article is organized as follows. In Sect. II general relations among the current, helicity amplitudes, and transition form factors are given. Formalisms, wave functions, and explicit expressions for the transition form factors are presented in Sect. III. In Sect. IV numerical results are presented, and a comparison is made with the lattice simulation data. Furthermore, meson cloud contributions are estimated in the present approach. Finally, discussions and conclusions are given in Sect. V.

## II. HELICITY AMPLITUDES AND FORM FACTORS

The electromagnetic transition between a nucleon (mass  $M$ ) and a spin 1/2 positive parity nucleon resonance  $N^*$  (mass  $M_R$ ) can be written using the Dirac  $F_1^*$  and Pauli  $F_2^*$  type form factors, defined by the current [7],

$$J^\mu = \bar{u}_R(P_+) \left\{ \left( \gamma^\mu - \frac{\not{q} q^\mu}{q^2} \right) F_1^* + \frac{i \sigma^{\mu\nu} q_\nu}{M_R + M} F_2^* \right\} u(P_-), \quad (1)$$

where,  $u_R$  ( $u$ ) is the  $N^*$  (nucleon) Dirac spinor,  $P_+$  ( $P_-$ ) is the final (initial) momentum and  $q = P_+ - P_-$ . Spin projection indices are suppressed for simplicity.

Usually, experimental data measured for hadron electromagnetic structure are reported in terms of the helicity amplitudes in a particular frame. The most popular choice is the rest frame of the final state, projecting the current on the photon polarization states,  $\varepsilon_\lambda^\mu$ , where  $\lambda = 0, \pm$  is the photon spin projection. In the  $N^*$  rest frame, the helicity amplitudes,  $A_{1/2}$  and  $S_{1/2}$ , are given by [4, 7, 8]:

$$A_{1/2}(Q^2) = \mathcal{K} \frac{1}{e} \langle N^*, +\frac{1}{2} | \varepsilon_+ \cdot J | N, -\frac{1}{2} \rangle, \quad (2)$$

$$S_{1/2}(Q^2) = \mathcal{K} \frac{1}{e} \langle N^*, +\frac{1}{2} | \varepsilon_0 \cdot J | N, +\frac{1}{2} \rangle \frac{|\mathbf{q}|}{Q}. \quad (3)$$

Here,  $e = \sqrt{4\pi\alpha}$  is the magnitude of the electron charge with  $\alpha \simeq 1/137$ , and

$$\mathcal{K} = \sqrt{\frac{2\pi\alpha}{K}}, \quad (4)$$

with  $K = \frac{M_R^2 - M^2}{2M_R}$ .  $|\mathbf{q}|$  is the photon momentum in the  $N^*$  rest frame,

$$|\mathbf{q}| = \frac{\sqrt{Q_+^2 - Q_-^2}}{2M_R}, \quad (5)$$

where  $Q_\pm^2 = (M_R \pm M)^2 + Q^2$ , with  $Q^2 = -q^2$ .

The helicity amplitudes,  $A_{1/2}$  and  $S_{1/2}$ , can be related with the form factors  $F_1^*$  and  $F_2^*$  via Eqs. (1)-(3) [4, 7, 8]:

$$A_{1/2}(Q^2) = \mathcal{R} \{ F_1^*(Q^2) + F_2^*(Q^2) \}, \quad (6)$$

$$S_{1/2}(Q^2) = \frac{\mathcal{R}}{\sqrt{2}} |\mathbf{q}| \frac{M_R + M}{Q^2} \{ F_1^*(Q^2) - \tau F_2^*(Q^2) \}, \quad (7)$$

where  $\tau = \frac{Q^2}{(M_R + M)^2}$ , and

$$\mathcal{R} = \sqrt{\frac{\pi\alpha Q_-^2}{M_R M K}}. \quad (8)$$

Note that the amplitude  $S_{1/2}$  is determined by virtual photons and not specified at  $Q^2 = 0$ , but obtained only in the limit  $Q^2 \rightarrow 0$ . In this case, one has

$$A_{1/2}(0) = \mathcal{R} F_2^*(0), \quad (9)$$

$$S_{1/2}(0) = \frac{\mathcal{R}}{\sqrt{2}} (M_R + M) K \left\{ \frac{dF_1^*}{dQ^2}(0) - \frac{F_2^*(0)}{(M_R + M)^2} \right\}. \quad (10)$$

The inverse relations for  $F_i^*$  ( $i = 1, 2$ ) in terms of the helicity amplitudes are:

$$F_1^*(Q^2) = \frac{1}{\mathcal{R}} \frac{\tau}{1 + \tau} \left\{ A_{1/2}(Q^2) + \sqrt{2} \frac{M_R + M}{|\mathbf{q}|} S_{1/2}(Q^2) \right\}, \quad (11)$$

$$F_2^*(Q^2) = \frac{1}{\mathcal{R}} \frac{1}{1 + \tau} \left\{ A_{1/2}(Q^2) - \sqrt{2} \frac{M_R + M}{|\mathbf{q}|} \tau S_{1/2}(Q^2) \right\}. \quad (12)$$

If the amplitudes  $A_{1/2}$  and  $S_{1/2}$  are finite at  $Q^2 = 0$ , Eq. (11) implies that

$$F_1^*(0) = 0. \quad (13)$$

As for  $F_2^*(0)$ , there is no particular condition.

For the Roper a fit to the data suggests a small value for  $S_{1/2}(0)$  [7]. Thus, at low  $Q^2$ ,  $F_1^*$  and  $F_2^*$  are determined essentially by  $A_{1/2}(Q^2)$ .

## III. FORM FACTORS IN A VALENCE QUARK MODEL

So far, a covariant spectator quark model has been developed and applied successfully to the spin 1/2 [11, 44] and 3/2 [39–43] ground states with no radial excitations. In the model, a three-quark baryon is described as an isolated quark which interacts with a photon, and a spectator diquark. The wave function of a baryon is represented in terms of the flavor and spin states of the quark and diquark combined with the relative angular momentum. In the spirit of the covariant spectator theory the quark pair degrees of freedom are integrated out to form an on-shell diquark with a certain mass  $m_D$ .

### A. Baryon wave functions

To describe the momentum distribution of the quark-diquark system in a baryon  $B$ , we introduce a scalar wave function  $\psi_B$ , which depends on the relative angular momentum and the radial excitation of the system. As the baryon and the diquark are on-shell the scalar wave function  $\psi_B$  can be written as a function of  $(P - k)^2$  [11], where  $P$  is the baryon total momentum and  $k$  the diquark momentum. We represent that dependence in term of the dimensionless variable [11],

$$\chi_B = \frac{(M_B - m_D)^2 - (P - k)^2}{M_B m_D}, \quad (14)$$

where  $B$  is the baryon index ( $B = N, \Delta, N^*$ , etc) and  $M_B$  the mass.

The nucleon wave function,  $\Psi_N(P, k)$ , can be written in the simplest S-wave model [11]:

$$\Psi_N(P, k) = \frac{1}{\sqrt{2}} [\phi_I^0 \phi_S^0 + \phi_I^1 \phi_S^1] \psi_N(P, k), \quad (15)$$

where  $\phi_{I,S}^{0,1}$  represents isospin ( $I$ ) or spin ( $S$ ) states corresponding to the total magnitude of either 0 or 1 in the diquark configuration [11]. (See Appendix A for the detail.) The wave function represented by Eq. (15), satisfies the Dirac equation [11, 39]. The scalar wave function  $\psi_N$  (S-state) is given by,

$$\psi_N(P, k) = \frac{N_0}{m_D(\beta_1 + \chi_N)(\beta_2 + \chi_N)}, \quad (16)$$

where  $\chi_N$  is obtained by inserting  $M_B = M$  in Eq. (14), and  $N_0$  the normalization constant. In a parameterization where  $\beta_1 > \beta_2$ ,  $\beta_1$  is associated with the long range physics, while  $\beta_2$  the short range physics.

In the present approach, the spin and isospin of the Roper are the same as those of the nucleon. Assuming the Roper to be the first radial excitation of the nucleon, we can write the Roper scalar wave function  $\psi_R$  as

$$\begin{aligned} \psi_R(P, k) &= N_R \frac{\beta_3 - \chi_R}{(\beta_1 + \chi_R)} \\ &\times \frac{1}{m_D(\beta_1 + \chi_R)(\beta_2 + \chi_R)}, \end{aligned} \quad (17)$$

where  $\beta_3$  is a new parameter which will be discussed later, and  $N_R$  the normalization constant. The sign of the normalization constant can be fixed by the experimental data [8]. This particular form with the order one polynomial in  $\chi_R$  (as  $\beta_3 - \chi_R$ ), is motivated by the harmonic-oscillator potential model for the three-quark system. A similar dependence was adopted in Ref. [17].

Note that the wave function represented by Eq. (17) preserves the short range behavior as presented in the nucleon scalar wave function, and that it simultaneously modifies the long range properties through the factor  $\frac{\beta_3 - \chi_R}{(\beta_1 + \chi_R)}$ . The Roper wave function  $\Psi_R$  also satisfies the Dirac equation with mass  $M_R$ .

The parameter  $\beta_3$  in the Roper scalar wave function in Eq. (17), will be fixed by the orthogonality condition between the nucleon and the Roper states.  $N_R$  will be fixed by  $\int_k |\psi_R|^2 = 1$  at  $Q^2 = 0$ , the same as that for the nucleon [11]. Thus, the description of the Roper requires no extra parameters to be fixed for the present purpose, since the parameters  $\beta_1$  and  $\beta_2$  have already been fixed [11].

### B. Transition form factors

In the covariant spectator quark model the transition current for the  $\gamma N \rightarrow P_{11}(1440)$  reaction can be written in a relativistic impulse approximation [11, 39, 40],

$$J^\mu = 3 \sum_\lambda \int_k \bar{\Psi}_R(P_+, k) j_I^\mu \Psi_N(P_-, k), \quad (18)$$

where  $\int_k \equiv \int \frac{d^3k}{2E_D(2\pi)^3}$  with  $E_D$  the diquark on shell energy,  $P_+ - P_- = q$  ( $Q^2 = -q^2$ ), and  $j_I^\mu$  is the quark current parameterized as

$$j_I^\mu = j_1(Q^2) \gamma^\mu + j_2(Q^2) \frac{i\sigma^{\mu\nu} q_\nu}{2M}. \quad (19)$$

The Dirac ( $j_1$ ) and Pauli ( $j_2$ ) quark form factors in the above are also decomposed as

$$j_i(Q^2) = \frac{1}{6} f_{i+}(Q^2) + \frac{1}{2} f_{i-}(Q^2) \tau_3, \quad (i = 1, 2). \quad (20)$$

The quark form factors  $f_{i\pm}$  are normalized as  $f_{1\pm}(0) = 1$  and  $f_{2\pm}(0) = \kappa_\pm$  (isoscalar and isovector quark anomalous moments). Their explicit expressions can be found in Refs. [11, 39, 40] and in Appendix A.

Using the expressions for the nucleon and Roper wave functions, Eqs. (15)-(17), and the hadronic current, Eq. (18), one gets explicit expressions for  $F_1^*(Q^2)$  and  $F_2^*(Q^2)$ :

$$\begin{aligned} F_1^*(Q^2) &= \frac{3}{2} j_1 \mathcal{I} + \frac{1}{2} \frac{3(M_R + M)^2 - Q^2}{(M_R + M)^2 + Q^2} j_3 \mathcal{I} \\ &\quad - \frac{M_R + M}{M} \frac{Q^2}{(M_R + M)^2 + Q^2} j_4 \mathcal{I}, \end{aligned} \quad (21)$$

$$\begin{aligned} F_2^*(Q^2) &= \frac{3}{4} \frac{M_R + M}{M} j_2 \mathcal{I} - \frac{(M_R + M)^2}{(M_R + M)^2 + Q^2} j_3 \mathcal{I} \\ &\quad + \frac{M_R + M}{2M} \frac{(M_R + M)^2 - 3Q^2}{(M_R + M)^2 + Q^2} j_4 \mathcal{I}, \end{aligned} \quad (22)$$

where  $\mathcal{I}(Q^2)$  is the overlap integral for the Roper and nucleon scalar wave functions:

$$\mathcal{I}(Q^2) = \int_k \psi_R(P_+, k) \psi_N(P_-, k), \quad (23)$$

and

$$\begin{aligned} j_{(i+2)} &= \frac{1}{3} \tau_3 j_i \tau_3 \\ &= \frac{1}{6} f_{i+}(Q^2) - \frac{1}{6} f_{i-}(Q^2) \tau_3, \quad (i = 1, 2). \end{aligned} \quad (24)$$

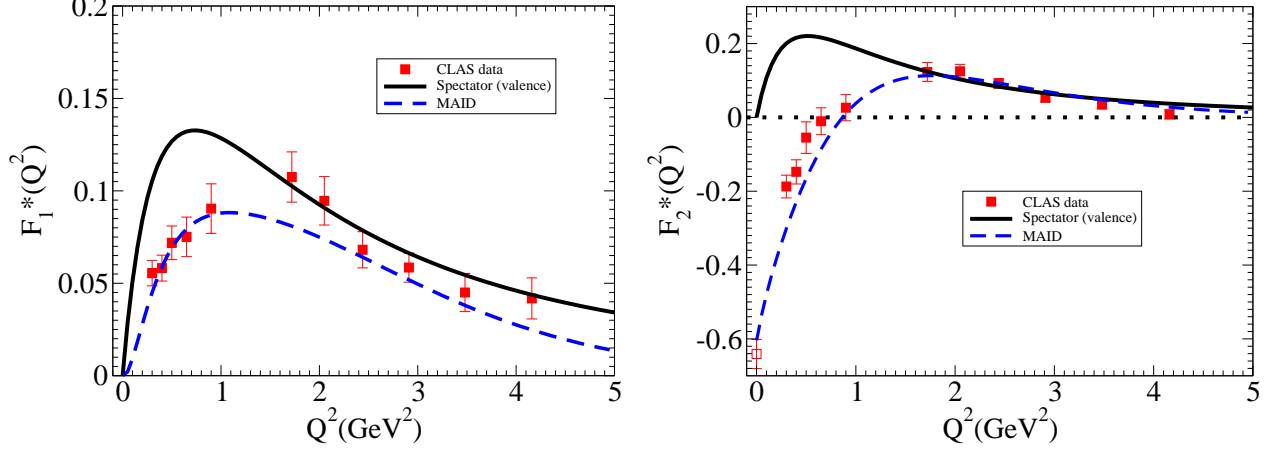


FIG. 1: Valence quark contributions (solid lines) calculated in the present model for  $F_1^*$  and  $F_2^*$ . The CLAS data [5] (squares with errorbars) and the MAID fit (dashed lines) are also shown. The result for  $F_2^*(0)$  is obtained from the PDG result [46] by converting the  $A_{1/2}(0)$ . (See Eq. (9).)

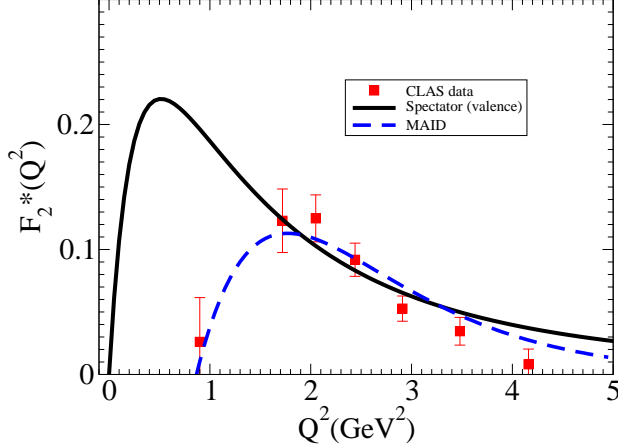


FIG. 2: Valence quark contributions for  $F_2^*$ , but partly magnified from Fig. 1. See also the caption of Fig. 1.

Equations (21)-(22) are the main expressions of the present model for the transition form factors. At  $Q^2 = 0$ , one has

$$\begin{aligned} F_1^*(0) &= \frac{3}{2}(j_1 + j_3)\mathcal{I}(0), \\ &= \frac{1}{2}(1 + \tau_3)\mathcal{I}(0). \end{aligned} \quad (25)$$

In this case, the desired result,  $F_1^*(0) = 0$ , is ensured only if  $\mathcal{I}(0) = 0$ . But this is indeed fulfilled by the orthogonality condition between the nucleon and the Roper wave functions. More detail will be discussed in next section.

### C. Orthogonality condition between the nucleon and the Roper states

The orthogonality condition between the nucleon and the Roper states in the present approach is:

$$\mathcal{I}(0) = \int_k \psi_R(\bar{P}_+, k) \psi_N(\bar{P}_-, k) = 0. \quad (26)$$

This can be regarded as a generalization of the nonrelativistic orthogonality condition when  $Q^2 = 0$  in the final Roper rest frame, namely,  $\bar{P}_+ = (M_R, 0, 0, 0)$  and  $\bar{P}_- = \left(\frac{M_R^2 + M^2}{2M_R}, 0, 0, -\frac{M_R^2 - M^2}{2M_R}\right)$ . In Appendix B, we discuss more on Eq. (26) and the nonrelativistic orthogonality condition. Note that the condition Eq. (26) is not automatically verified for the nucleon and the Roper wave functions in Eqs. (16)-(17). The orthogonality condition is satisfied only for a particular value of  $\beta_3$  that sets  $\mathcal{I}(0) = 0$ .

A direct consequence of the orthogonality condition Eq. (26), is that  $F_1^*(0) = 0$ , and also that  $F_2^*(0) = 0$ .  $F_1^*(0) = 0$  is consistent with the general properties of the  $\gamma N \rightarrow P_{11}(1440)$  reaction.  $F_2^*(0) = 0$  is a prediction of our model as a consequence of the orthogonality condition Eq. (26), but it also corresponds to an approximation, since the sea quark contributions are ignored in the present approach. A more accurate treatment would give a small value for  $|F_2^*(0)|$ .

## IV. RESULTS

The nucleon and the Roper wave functions are described by Eq. (15) with their scalar functions, Eqs. (16)-(17). The parameters for the Roper wave function are determined by those of the nucleon [11]:  $\beta_1 = 0.049$  and

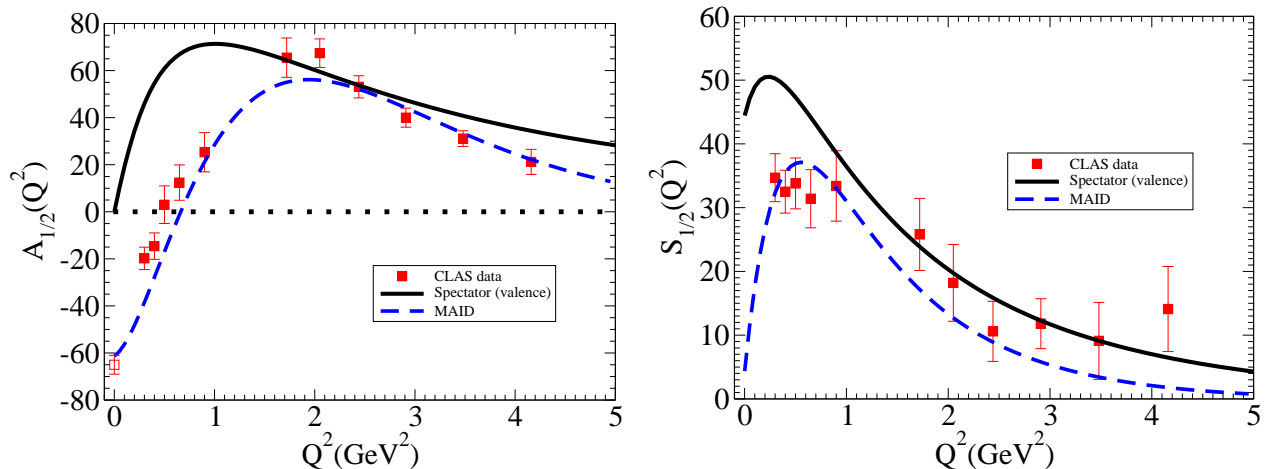


FIG. 3: Valence quark contributions for the  $A_{1/2}$  and  $S_{1/2}$  helicity amplitudes. The CLAS data [5] and the MAID fit are also shown [7]. See also the caption of Fig. 1.

$\beta_2 = 0.717$ , and by the orthogonality condition Eq. (26) to give  $\beta_3 = 0.130$  and  $N_R = 3.35$ .

#### A. Results for $F_1^*$ and $F_2^*$

Before presenting the results, we emphasize again that there are no new free parameters to be fixed in the model. Thus, for a given  $Q^2$ , the form factors can be calculated using Eqs. (21)-(22). The valence quark contributions calculated in the present model for the  $F_1^*$  and  $F_2^*$  form factors are shown in Fig. 1 by the solid lines. In Fig. 2 also a part magnified from Fig. 1 for  $F_2^*$  is shown. The magnitudes of the present results are consistent with constituent and light-front quark models [4, 5, 17]. For convenience, we present in Fig. 3 the helicity amplitudes calculated in the Roper rest frame, using the relations Eqs. (6)-(7).

In Fig. 1 we also compare the valence quark contributions with the CLAS data for  $F_1^*$  and  $F_2^*$ . The CLAS data were extracted combining dispersion relations with a Unitary Isobar Model analysis [5]. As one can see our result is very close to the data in the region  $Q^2 > 1.5 \text{ GeV}^2$  (see especially Fig. 2 for  $F_2^*$ ), which supports the idea that the meson cloud contributions are suppressed in the high  $Q^2$  region, and the assumption that the Roper is the first radial excitation of the nucleon. This achievement may be impressive since we have introduced no extra new parameters as already mentioned. One only may identify the long range behavior of the Roper wave function with that of the nucleon, and may ensure the orthogonality between the Roper and the nucleon wave functions. In Fig. 1 we also show a fit to the data from Ref. [6], using the code MAID2007 (abbreviated MAID) [7]. Both the CLAS data and the MAID fit are similar for  $Q^2 > 2 \text{ GeV}^2$  region, although some differences may be noticeable, in particular for  $F_1^*$ . This discrepancy in  $F_1^*$  can be

also a consequence of the different data sets used in the analysis between the CLAS data and the MAID fit. Our predictions for  $F_1^*$  are closer to the CLAS analysis than to the MAID fit, although the differences are comparable with the errorbars of the CLAS data.

Next, we discuss the asymptotic behavior for  $F_1^*$  and  $F_2^*$  as  $Q^2 \rightarrow \infty$ . Perturbative QCD (pQCD) [47, 48] predicts  $F_1^*(Q^2) \sim 1/Q^4$  and  $F_2^*(Q^2) \sim 1/Q^6$  as  $Q^2 \rightarrow \infty$ , apart from the  $\log Q^2$  corrections. The predictions of the present model from Eqs. (21)-(22), are consistent with these results:  $F_1^*(Q^2) \simeq 1.21 \mathcal{I}$  and  $F_2^*(Q^2) \simeq 13.1 \frac{\mathcal{I}}{Q^2}$ , with  $\mathcal{I} = \mathcal{O}(\log Q^2)/Q^4$ . (See Appendix G of Ref. [39] for details.) For the helicity amplitudes, our results are also consistent with the pQCD predictions<sup>1</sup>:  $A_{1/2}, S_{1/2} \sim 1/Q^3$  [47, 48], again apart from the logarithmic corrections. Note, however, that based on what observed for the nucleon [11], and especially for the  $\gamma N \rightarrow \Delta$  transition form factors [40], the predicted scaling behaviors may not be observed in such a small  $Q^2$  region. Also it is not realistic to expect that our calibration of the quark current based on the reactions in the regime  $Q^2 < 6 \text{ GeV}^2$ , can be naively extended to the high  $Q^2$  region where pQCD is valid (such as  $Q^2 \sim 100 - 1000 \text{ GeV}^2$ ).

<sup>1</sup> From Refs. [47, 48] one has

$$G_+ \sim 1/Q^3, \quad G_0 \sim 1/Q^4, \quad (27)$$

where  $G_+ = A_{1/2}$  and  $G_0 = \frac{Q}{|q|} S_{1/2}$ . Note that the extra power in  $G_0$  in contrast to  $G_+$ . This takes account of changing the helicity one unit between the initial and final states [47, 48]. Thus, one gets,  $A_{1/2} \sim 1/Q^3$  and  $S_{1/2} \sim 1/Q^3$ .

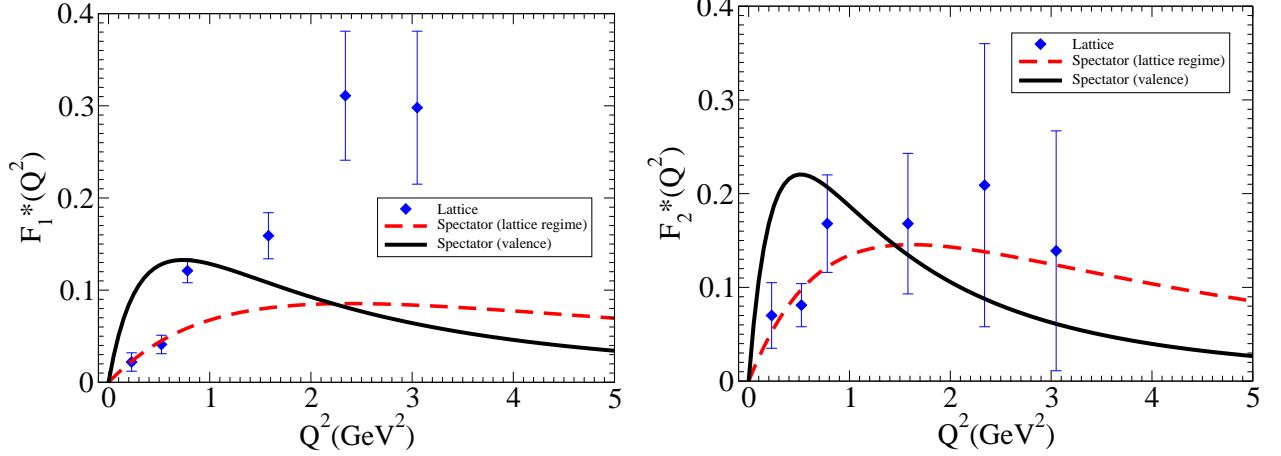


FIG. 4: Valence quark contributions in the lattice regime (dashed lines) corresponding to the pion mass  $m_\pi = 720$  MeV. The lattice data with  $m_\pi = 720$  MeV (diamonds) are from Ref. [37]. The solid lines are the valence quark contributions calculated with the physical pion mass,  $m_\pi = 138$  MeV. The mass values used corresponding to the lattice regime ( $m_\pi = 720$  MeV) for the nucleon, Roper and  $\rho$  meson are,  $M = 1.48$  GeV,  $M_R = 2.53$  GeV, and  $m_\rho = 1.083$  GeV, respectively.

### B. Comparing with the lattice results

Extending the model to the lattice simulation regime, we compare our results with the lattice QCD results. Hereafter, the results obtained in the lattice regime will be referred to as "lattice regime", which will be explained below. One can expect that, the heavier the pion mass becomes in the lattice simulations, the closer our results become to the lattice one, since the meson cloud effects become smaller. A comparison is made in Fig. 4 for the lattice data corresponding to  $m_\pi = 720$  MeV [37]. To extend the model to the lattice regime, we include an implicit dependence on the pion mass for the hadron masses, following the procedure proposed in Refs. [49, 50]. This is done by replacing the hadron masses in the baryon wave function and the quark electromagnetic current [Eq. (19)]. In the lattice regime (the dashed lines in Fig. 4) we have used the nucleon and the Roper masses,  $M = 1.48$  GeV and  $M_R = 2.53$  GeV, respectively, corresponding to the pion mass  $m_\pi = 720$  MeV [37]. We have also used the value, 1.083 GeV for the  $\rho$  meson mass, according to the parameterization in Ref. [51].

One can see in Fig. 4 that the lattice regime results are fairly consistent with the lattice data for  $F_2^*$ . As for  $F_1^*$ , the lattice results overestimate our predictions for  $Q^2 > 1.5$  GeV<sup>2</sup>, as well as the covariant spectator model results "Spectator (valence)" (the same as those shown in Figs. 1 and 2). However, for  $Q^2 < 0.6$  GeV<sup>2</sup>, the agreement is excellent. More lattice QCD simulation data with smaller pion masses are desired to constrain better the valence quark contributions in the low  $Q^2$  region. The agreement between the lattice regime results and the lattice QCD data, supports that the present estimate of the valence quark contributions is reasonable.

### C. Estimating the meson cloud effects

To estimate the meson cloud effects, we take the valence quark contributions estimated in subsection IV A as a reference. The valence quark contributions will be denoted by  $F_i^{bare}(i = 1, 2)$ . We need to know a full contribution to estimate the meson cloud contributions. As a first step approach, we regard the MAID fit results [6], which will be denoted by  $F_i^{MAID}(Q^2)(i = 1, 2)$ , as the total contribution for the form factors. Then, the meson cloud contributions  $F_i^{mc}$ , may be estimated by

$$F_i^{mc}(Q^2) = F_i^{MAID}(Q^2) - F_i^{bare}(Q^2), \quad (i = 1, 2). \quad (28)$$

The results for  $F_i^{mc}$  are presented in Fig. 5. To have an idea for the uncertainties in this estimate we use an analytical form for the each form factor upper limit of the CLAS data errorbars [denoted by  $\sigma(F_i^*)(i = 1, 2)$  below], and calculate the bands with one-standard deviation. Specifically, we use  $\sigma(F_1^*) \simeq 0.015(1 - e^{-3Q^2})$  and  $\sigma(F_2^*) \simeq 0.05 - 0.009Q^2$ .

First, we analyze  $F_1^*$ . A situation for  $F_1^*$  is a bit subtle. The magnitude of the data is smaller than that of the  $F_2^*$ . The upper limit for  $|F_1^*|$  is around 0.1, which is about half of that for  $|F_2^*|$ . The meson cloud contributions are negative, and they can be between 0.01 to 0.03 in the high  $Q^2$  region. Probably, the contributions of 0.03 are overestimated, since they are expected to become small in the high  $Q^2$  region. We note however, the meson cloud contributions here are estimated by subtracting the model results from the MAID fit. There are differences in the CLAS data and the MAID fit in the high  $Q^2$  region, since the MAID analysis [5] uses a different data set from that of the CLAS [5]. The clarification between the differences in the two data sets, and more precision data in this high  $Q^2$  region (less contaminations from meson

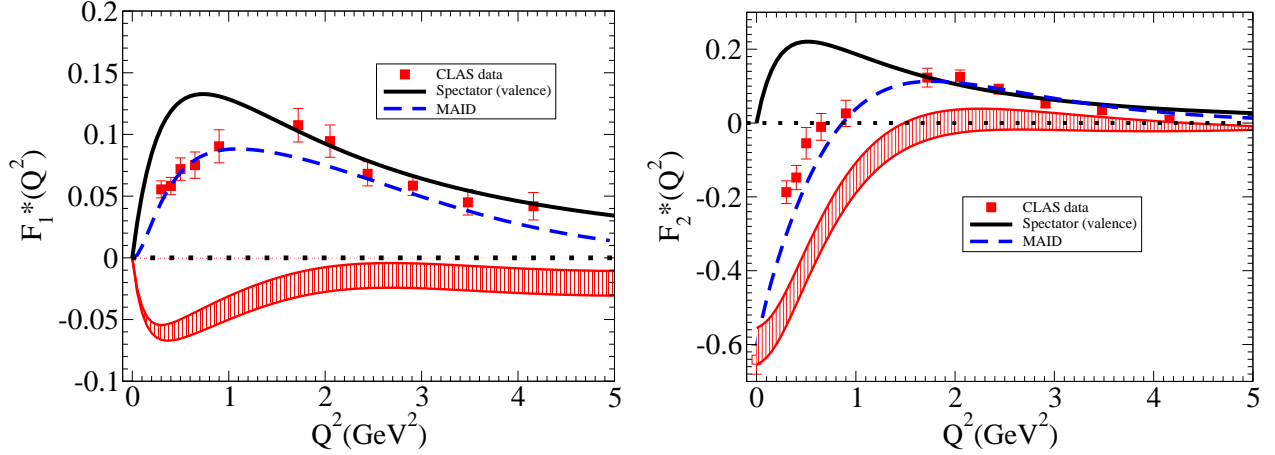


FIG. 5: Meson cloud contributions (shaded areas) for  $F_1^*$  (left panel) and  $F_2^*$  (right panel). The bands are estimated by the upper limits of the CLAS errorbars:  $\sigma(F_1^*) = 0.015(1 - e^{-3Q^2})$  and  $\sigma(F_2^*) = 0.05 - 0.009Q^2$ , with one-standard deviation.

cloud), are desired to constrain better the meson cloud contributions for  $F_1^*$ .

Next we discuss  $F_2^*$ . Due to the larger magnitude of  $F_2^*$ , the contributions from the meson cloud may be easier to estimate. The meson cloud contributions for  $F_2^*$  are negative as well as those for  $F_1^*$ . As one can see in Fig. 5 the meson cloud gives main contributions in the low  $Q^2$  region. (At  $Q^2 = 0$ , they are the only contributions.) However, as expected, the meson cloud contributions become small for  $Q^2 > 1.5 \text{ GeV}^2$ , and the valence quark contributions dominate. In higher  $Q^2$  region, the magnitude of the meson cloud contributions are of order of the errorbars ( $\sim 0.01$ ) of the data.

Overall, our estimate of the meson cloud contributions qualitatively agree with those of the recent works [10, 20, 23, 29], particularly for  $F_1^*$ .

Finally, in terms of the helicity amplitudes the meson cloud contributions at  $Q^2 = 0$  are estimated by  $A_{1/2}^{mc}(0) = (-61.4 \pm 4.9) \times 10^{-3} \text{ GeV}^{-1/2}$  and  $S_{1/2}^{mc}(0) = (-40.2 \pm 2.6) \times 10^{-3} \text{ GeV}^{-1/2}$ . Meson cloud is the only contributions for  $A_{1/2}(0)$ . As for  $S_{1/2}(0)$ , the meson cloud contributions cancel significantly with those of the valence quark. This feature can be understood better by observing Fig. 3.

## V. CONCLUSIONS

In this work we have studied the transition form factors for  $\gamma N \rightarrow P_{11}(1440)$  reaction using a covariant spectator quark model. The model is fully relativistic, and has no new adjustable parameters. This is fulfilled by the orthogonality condition between the nucleon and the Roper states. The model can describe the reaction well in the high  $Q^2$  region ( $1.5 \text{ GeV}^2 < Q^2 < 4.0 \text{ GeV}^2$ ), supporting the idea that the Roper is the first radial excitation of the nucleon. In the low  $Q^2$  region ( $Q^2 < 1.5 \text{ GeV}^2$ ) the model

predictions deviate from the experimental data, and this fact suggests that the meson cloud contributions (missing in the model) are significant in this  $Q^2$  region.

To check whether or not the description of our estimate for the valence quark contributions is realistic, we have extended the model to the lattice regime to compare with the heavy-pion lattice QCD data. Our results are in an excellent agreement with them in the low  $Q^2$  region. This fact supports that the valence quark degrees of freedom is well described in our model. Having a good confidence in the description of the valence quark sector, we have estimated the meson cloud contributions for the Dirac ( $F_1^*$ ) and Pauli ( $F_2^*$ ) type transition form factors. A characteristic feature of the model,  $F_2^*(0) = 0$ , is a direct consequence of the orthogonality condition between the nucleon and the Roper states. However, this may not have significant consequences in the estimate of the meson cloud contributions, since they appear to be dominant at low  $Q^2$ , or conversely, the valence quark contributions are expected to be small at  $Q^2 = 0$  [4].

In this work we have shown that the transition form factors  $F_1^*$  and  $F_2^*$  for the  $\gamma N \rightarrow P_{11}(1440)$  reaction may be more suitable quantities to study than the helicity amplitudes in order to disentangle the meson cloud contributions. For example,  $|F_1^*|$  is small for both in experimental data and the valence quark model because of the cancellation between the  $A_{1/2}$  and  $S_{1/2}$  amplitudes. This implies also the meson cloud contributions are small. As for  $F_2^*$ , it is mainly determined by  $A_{1/2}(Q^2)$  in the very low  $Q^2$  region, which measures the meson cloud contributions in our approach (for  $Q^2 \rightarrow 0$ ).

We admit that our estimate of the meson cloud contributions has some limitations due to the parameterization of the amplitudes  $A_{1/2}$  and  $S_{1/2}$  based on the MAID analysis. Furthermore, we have faced that there are some discrepancies between the two data sets of the CLAS and MAID in the high  $Q^2$  region. More precision experimen-



tal data in this high  $Q^2$  region are desired to constrain better the meson cloud contributions.

For a possible improvement, there is a room to add one extra free parameter to the model. The parameter  $\beta_1$  (fixed by the nucleon wave function) in the factor  $\frac{\beta_3 - \chi_R}{\beta_1 + \chi_R}$  in the Roper wave function, can be replaced by a new free parameter  $\beta_4$  to introduce a new long range scale, and may be adjusted by more precise, high  $Q^2$  data. Needless to say, more lattice QCD data are also useful to constrain the valence quark contributions better.

We plan to extend the present model for higher mass resonance region, like for instance,  $S_{11}(1535)$ . In the past dynamical coupled-channel models are very successful in the description of the meson-baryon electro- and photoreaction, involving resonances such as  $\Delta(1232)$ ,  $P_{11}(1440)$  and  $S_{11}(1535)$ . However, such models require a parameterization in the interaction with the quark core. In general, it is based on the baryon-meson phenomenology and not based on the quark (and gluon) degrees of freedom. The approach developed in this work is very promising to study the valence quark contributions in the meson-baryon systems. It can be tested, or compared with the bare parameters used in the dynamical coupled-channel models. An independent test may be to compare with the 'bare' contributions (no meson cloud) determined by dynamical meson-baryon coupled channel models by fitting e.g., to the cross section data at each  $Q^2$  [26–28]. This kind of an extraction of the 'bare' contributions was done for the  $\gamma N \rightarrow \Delta$  reaction [26], as well as other resonances including the Roper [27, 28]. However, often the meson cloud contributions become larger than the quark core contributions, and an estimate of the bare contributions are sometimes difficult to get as a smooth function of  $Q^2$ . Another possible method is to use the lattice QCD data in the heavy-pion regime to fix the valence quark contributions. This method was successfully applied in Ref. [50] for the nucleon to  $\Delta$  electromagnetic transition.

### Acknowledgments:

The authors thank B. Juliá-Díaz, H. Kamano, M. T. Peña, A. Sibirtsev, A. Stadler for helpful discussions, and A. W. Thomas for suggestions in the manuscript. This work was support by Jefferson Science Associates, LLC under U.S. DOE Contract No. DE-AC05-06OR23177, and in part by the European Union (HadronPhysics2 project “Study of strongly interacting matter”). G. R. was also supported by the Portuguese Fundação para a Ciência e Tecnologia (FCT) under the grant SFRH/BPD/26886/2006. K. T. acknowledges the CSSM (Adelaide, Australia) for a hospitality, where this work was completed.

### Appendix A: Covariant spectator quark model

Below, we present some details of the covariant spectator quark model.

### 1. Wave functions

In the covariant spectator quark model the S-state wave function for the nucleon with the (initial) momentum  $P_-$  is given by [11],

$$\Psi_N(P_-, k) = \frac{1}{\sqrt{2}} \left[ \phi_I^0 u(P_-) - \phi_I^1 \varepsilon_{P_-}^\alpha U_\alpha(P_-) \right] \psi_N(P_-, k), \quad (A1)$$

where  $k$  is the diquark momentum and  $\phi_I^{0,1}$  is the combination of the quark flavors associated with the isospin 0 or 1 diquark. The spin-1 polarization vector is represented by  $\varepsilon_{P_-}$  in a Fixed-Axis base [52], and  $u$  and  $U^\alpha$  are the spinors related by [39],

$$U^\alpha(P) = \frac{1}{\sqrt{3}} \gamma_5 \left( \gamma^\alpha - \frac{P^\alpha}{M} \right) u(P). \quad (A2)$$

The Roper wave function with the (final) momentum  $P_+$  is defined by

$$\Psi_R(P_+, k) = \frac{1}{\sqrt{2}} \left[ \phi_I^0 u_R(P_+) - \phi_I^1 \varepsilon_{P_+}^{\prime\alpha} U'_\alpha(P_+) \right] \psi_R(P_+, k), \quad (A3)$$

where  $u_R$  and  $U'_\alpha$  are spin states associated with a spin 1/2 particle and mass  $M_R$ , and  $\varepsilon_{P_+}^\alpha$  is the polarization vector.

In both cases the scalar functions,  $\psi_N(P_-, k)$  and  $\psi_R(P_+, k)$ , are the functions of  $(P_- - k)^2$  and  $(P_+ - k)^2$ , respectively.

### 2. Quark form factors

The quark current associated with Eqs. (19) and (20) is expressed in terms of the quark form factors  $f_{i\pm}$  ( $i = 1, 2$ ), inspired by a vector meson dominance form:

$$f_{1\pm}(Q^2) = \lambda + (1 - \lambda) \frac{m_v^2}{m_v^2 + Q^2} + c_\pm \frac{M_h^2 Q^2}{(M_h^2 + Q^2)^2}, \quad (A4)$$

$$f_{2\pm}(Q^2) = \kappa_\pm \left\{ d_\pm \frac{m_v^2}{m_v^2 + Q^2} + (1 - d_\pm) \frac{M_h^2}{M_h^2 + Q^2} \right\}. \quad (A5)$$

In the above,  $\lambda$  defines the quark charge in deep inelastic scattering,  $\kappa_\pm$  are the isoscalar and isovector quark anomalous magnetic moments. The mass  $m_v$  ( $M_h$ ) corresponds to the light (heavy) vector meson, and  $c_\pm$ ,  $d_\pm$  are the mixture coefficients. In the present model we set  $m_v = m_\rho$  ( $\approx m_\omega$ ) for the light vectorial meson and  $M_h = 2M$  (twice the nucleon mass) to represent the short range physics. The values of the parameters were previously fixed by the nucleon elastic form factors [11], and the values are presented in Table I. Note that the present model uses  $d_+ = d_-$ .

### 3. Quark form factors and asymptotic expressions

In the present model, the asymptotic expressions for  $Q^2 \rightarrow \infty$ , associated with the quark current of Eqs. (20)



$\kappa_+$	$\kappa_-$	$c_+$	$c_-$	$d_+$	$d_-$	$\lambda$
1.639	1.823	4.16	1.16	-0.686	-0.686	1.21

TABLE I: Quark current parameters.

and (24) are given by

$$j_1 \simeq \frac{2}{3}\lambda, \quad (\text{A6})$$

$$j_3 \simeq \frac{1}{6}(c_+ - c_-) \frac{\mathcal{F}}{Q^2}, \quad (\text{A7})$$

$$j_2 \simeq \frac{1}{6}(\kappa_+ + 3\kappa_-) \frac{\mathcal{F}}{Q^2}, \quad (\text{A8})$$

$$j_4 \simeq \frac{1}{6}(\kappa_+ - \kappa_-) \frac{\mathcal{F}}{Q^2}, \quad (\text{A9})$$

with

$$\mathcal{F} = d_+ m_v^2 + (1 - d_+) M_h^2, \quad (\text{A10})$$

where, we have used the relation,  $d_+ = d_-$ , corresponding to the parameterization of the model II in Ref. [11]. In particular,  $\mathcal{F} = 5.54 \text{ GeV}^2$  should be noted.

Using Eqs. (A6)-(A9) we can derive the expressions for  $F_1^*$  and  $F_2^*$  for  $Q^2 \rightarrow \infty$ .

## Appendix B: The orthogonality of the nucleon and the Roper states

In a static, nonrelativistic formalism the wave function is a function of the particle's three-momentum,  $\mathbf{k}$ . In the limit where there is no momentum transfer, the arguments in the initial ( $\psi_i$ ) and final ( $\psi_f$ ) wave functions are the same. This corresponds to  $\mathbf{q} = \mathbf{k} - \mathbf{k} = 0$ , or  $Q^2 = -\mathbf{q}^2 = 0$ . Then, the overlap integral between the orthogonal states,  $\mathcal{I}$ , is given by

$$\int \frac{d^3\mathbf{k}}{(2\pi)^3} \psi_f^*(\mathbf{k}) \psi_i(\mathbf{k}) = 0. \quad (\text{B1})$$

The equivalent relation for the covariant spectator theory for Eq. (B1) is

$$\int_k \psi_f^*(P_+, k) \psi_i(P_-, k) \Big|_{Q^2=0} = 0, \quad (\text{B2})$$

where the sub-index  $Q^2 = 0$  indicates that  $Q^2 = -(P_+ - P_-)^2 = 0$ . The simplest case is in the initial (or

final) baryon's rest frame. For the equal mass case,  $P_+ = P_- = (M, 0, 0, 0)$ .

Next, consider the inelastic case with the masses of the initial and final states,  $M$  and  $M_R$ , respectively. The generalization of the condition Eq. (B2) would correspond to  $P_- = (M, 0, 0, 0)$  and  $P_+ = (M_R, 0, 0, 0)$ , with  $q = P_+ - P_- = \left(\frac{M_R^2 - M^2 - Q^2}{2M_R}, 0, 0, |\mathbf{q}|\right)$  when  $\mathbf{q} = \mathbf{0}$ . ( $|\mathbf{q}|$  is given by Eq. (5).) This gives also

$$Q^2 \equiv Q^{*2} = -(M_R - M)^2, \quad (\text{B3})$$

which will be denoted by the pseudo-threshold point, the point where both initial and final state are at rest. This situation is, however, unphysical for  $M_R \neq M$  because  $Q^2 < 0$ .

The generalization of Eq. (B2) for unequal mass case would be,

$$\int_k \psi_f^*(P_+, k) \psi_i(P_-, k) \Big|_{Q^2=Q^{*2}} = 0. \quad (\text{B4})$$

Since the physical reaction are restricted to  $Q^2 \geq 0$ , we need to redefine the orthogonality condition in the unequal mass case. To do so we impose the condition,

$$\int_k \psi_f^*(\bar{P}_+, k) \psi_i(\bar{P}_-, k) = 0, \quad (\text{B5})$$

where the four-momenta  $\bar{P}_+$  and  $\bar{P}_-$  are respectively defined by,

$$\begin{aligned} \bar{P}_- &= \left(\frac{M_R^2 + M^2}{2M_R}, 0, 0, -\frac{M_R^2 - M^2}{2M_R}\right), \\ \bar{P}_+ &= (M_R, 0, 0, 0), \end{aligned} \quad (\text{B6})$$

which correspond to  $Q^2 = 0$ , but  $\mathbf{q}^2 \neq 0$ .

The use of Eq. (B5) may be regarded as an approximation, or the simplest relativistic extension for the orthogonality condition. The exact treatment needs to impose the overlap integral to vanish at the pseudo-threshold as in Eq. (B4). However, it would require an extension of the wave functions to the unphysical region, and beyond a scope of the present study. Instead, we use Eq. (B5). Both prescriptions should give similar results when  $(M_R - M)^2$  is small enough.

- 
- [1] H. Clement *et al.*, arXiv:nucl-ex/0612015.  
[2] A. V. Sarantsev *et al.*, Phys. Lett. B **659**, 94 (2008) [arXiv:0707.3591 [hep-ph]].  
[3] N. Suzuki, B. Julia-Diaz, H. Kamano, T. S. Lee, A. Mat-

- suyama and T. Sato, arXiv:0909.1356 [nucl-th].  
[4] I. G. Aznauryan, Phys. Rev. C **76**, 025212 (2007) [arXiv:nucl-th/0701012].  
[5] I. G. Aznauryan *et al.* [CLAS Collaboration], Phys. Rev.

- C **80**, 055203 (2009) [arXiv:0909.2349 [nucl-ex]].
- [6] D. Drechsel, S. S. Kamalov and L. Tiator, Eur. Phys. J. A **34**, 69 (2007) [arXiv:0710.0306 [nucl-th]].
- [7] L. Tiator and M. Vanderhaeghen, Phys. Lett. B **672**, 344 (2009) [arXiv:0811.2285 [hep-ph]].
- [8] I. G. Aznauryan, V. D. Burkert and T. S. Lee, arXiv:0810.0997 [nucl-th].
- [9] V. D. Burkert, AIP Conf. Proc. **1056**, 348 (2008) [arXiv:0808.2326 [nucl-ex]].
- [10] B. Julia-Diaz, T. S. Lee, A. Matsuyama, T. Sato and L. C. Smith, Phys. Rev. C **77**, 045205 (2008) [arXiv:0712.2283 [nucl-th]].
- [11] F. Gross, G. Ramalho and M. T. Peña, Phys. Rev. C **77**, 015202 (2008) [arXiv:nucl-th/0606029].
- [12] Z. P. Li, Phys. Rev. D **44**, 2841 (1991); Z. P. Li, V. Burkert and Z. j. Li, Phys. Rev. D **46**, 70 (1992).
- [13] M. Warns, W. Pfeil and H. Rollnik, Phys. Rev. D **42**, 2215 (1990); M. Warns, H. Schroder, W. Pfeil and H. Rollnik, Z. Phys. C **45**, 627 (1990).
- [14] S. Capstick and B. D. Keister, Phys. Rev. D **51**, 3598 (1995) [arXiv:nucl-th/9411016].
- [15] F. Cardarelli, E. Pace, G. Salme and S. Simula, Phys. Lett. B **397**, 13 (1997) [arXiv:nucl-th/9609047].
- [16] M. M. Giannini, E. Santopinto and A. Vassallo, Eur. Phys. J. A **12**, 447 (2001) [arXiv:nucl-th/0111073].
- [17] B. Julia-Diaz, D. O. Riska and F. Coester, Phys. Rev. C **69**, 035212 (2004) [Erratum-ibid. C **75**, 069902 (2007)] [arXiv:hep-ph/0312169].
- [18] H. J. Weber, Phys. Rev. C **41**, 2783 (1990).
- [19] F. Cano and P. Gonzalez, Phys. Lett. B **431**, 270 (1998) [arXiv:nucl-th/9804071].
- [20] Q. B. Li and D. O. Riska, Phys. Rev. C **74**, 015202 (2006) [arXiv:nucl-th/0605076].
- [21] E. Santopinto and R. Bijker, Few Body Syst. **44**, 95 (2008).
- [22] M. Dillig and M. Schott, Phys. Rev. C **75**, 067001 (2007) [Erratum-ibid. C **76**, 019903 (2007)] [arXiv:nucl-th/0405063].
- [23] B. Julia-Diaz and D. O. Riska, Nucl. Phys. A **780**, 175 (2006) [arXiv:nucl-th/0609064].
- [24] O. Krehl, C. Hanhart, S. Krewald and J. Speth, Phys. Rev. C **62**, 025207 (2000) [arXiv:nucl-th/9911080].
- [25] B. Julia-Diaz, T. S. Lee, A. Matsuyama and T. Sato, Phys. Rev. C **76**, 065201 (2007) [arXiv:0704.1615 [nucl-th]].
- [26] B. Julia-Diaz, T. S. Lee, T. Sato and L. C. Smith, Phys. Rev. C **75**, 015205 (2007) [arXiv:nucl-th/0611033].
- [27] B. Julia-Diaz, H. Kamano, T. S. Lee, A. Matsuyama, T. Sato and N. Suzuki, Phys. Rev. C **80**, 025207 (2009) [arXiv:0904.1918 [nucl-th]].
- [28] N. Suzuki, T. Sato and T. S. Lee, arXiv:0910.1742 [nucl-th].
- [29] B. Golli, S. Sirca and M. Fiolhais, Eur. Phys. J. A **42**, 185 (2009) [arXiv:0906.2066 [nucl-th]].
- [30] B. Golli and S. Sirca, Few Body Syst. **44**, 157 (2008).
- [31] S. Schneider, S. Krewald and U. G. Meissner, Eur. Phys. J. A **28**, 107 (2006) [arXiv:nucl-th/0603040].
- [32] S. S. Kamalov, S. N. Yang, D. Drechsel, O. Hanstein and L. Tiator, Phys. Rev. C **64**, 032201(R) (2001) [arXiv:nucl-th/0006068].
- [33] V. D. Burkert and T. S. H. Lee, Int. J. Mod. Phys. E **13**, 1035 (2004) [arXiv:nucl-ex/0407020].
- [34] K. Bermuth, D. Drechsel, L. Tiator and J. B. Seaborn, Phys. Rev. D **37**, 89 (1988).
- [35] Y. B. Dong, K. Shimizu, A. Faessler and A. J. Buchmann, Phys. Rev. C **60**, 035203 (1999).
- [36] D. Y. Chen and Y. B. Dong, Commun. Theor. Phys. **50**, 142 (2008).
- [37] H. W. Lin, S. D. Cohen, R. G. Edwards and D. G. Richards, Phys. Rev. D **78**, 114508 (2008) [arXiv:0803.3020 [hep-lat]].
- [38] F. Gross, Phys. Rev. **186**, 1448 (1969); F. Gross, J. W. Van Orden and K. Holinde, Phys. Rev. C **45**, 2094 (1992).
- [39] G. Ramalho, M. T. Peña and F. Gross, Eur. Phys. J. A **36**, 329 (2008) [arXiv:0803.3034 [hep-ph]].
- [40] G. Ramalho, M. T. Peña and F. Gross, Phys. Rev. D **78**, 114017 (2008) [arXiv:0810.4126 [hep-ph]].
- [41] G. Ramalho and M. T. Peña, J. Phys. G **36**, 085004 (2009) [arXiv:0807.2922 [hep-ph]]; G. Ramalho, M. T. Peña and F. Gross, Phys. Lett. B **678**, 355 (2009) [arXiv:0902.4212 [hep-ph]].
- [42] G. Ramalho, M. T. Peña and Franz Gross, work in preparation
- [43] G. Ramalho, K. Tsushima and F. Gross, Phys. Rev. D **80**, 033004 (2009) [arXiv:0907.1060 [hep-ph]].
- [44] F. Gross, G. Ramalho and K. Tsushima, arXiv:0910.2171 [hep-ph].
- [45] P. Wang, D. B. Leinweber, A. W. Thomas and R. D. Young, Phys. Rev. D **75**, 073012 (2007) [arXiv:hep-ph/0701082].
- [46] C. Amsler *et al.* [Particle Data Group], Phys. Lett. B **667**, 1 (2008).
- [47] C. E. Carlson, Phys. Rev. D **34**, 2704 (1986);
- [48] G. Sterman and P. Stoler, Ann. Rev. Nucl. Part. Sci. **47**, 193 (1997) [arXiv:hep-ph/9708370].
- [49] G. Ramalho and M. T. Peña, J. Phys. G **36**, 115011 (2009) [arXiv:0812.0187 [hep-ph]].
- [50] G. Ramalho and M. T. Peña, Phys. Rev. D **80**, 013008 (2009) [arXiv:0901.4310 [hep-ph]].
- [51] D. B. Leinweber, A. W. Thomas, K. Tsushima and S. V. Wright, Phys. Rev. D **64**, 094502 (2001) [arXiv:hep-lat/0104013].
- [52] F. Gross, G. Ramalho and M. T. Peña, Phys. Rev. C **77**, 035203 (2008).